

ULTRAVIOLET OBSERVATIONS OF THE PECULIAR SUPERNOVA REMNANT IN NGC 4449

WILLIAM P. BLAIR¹ AND JOHN C. RAYMOND¹
 Harvard-Smithsonian Center for Astrophysics

AND

ROBERT A. FESEN^{1,2} AND THEODORE R. GULL¹
 Laboratory for Astronomy and Solar Physics, NASA/Goddard Space Flight Center

Received 1983 May 24; accepted 1983 October 10

ABSTRACT

We have obtained *IUE* spectra of the emission region in the irregular galaxy NGC 4449 that has been identified as a young, oxygen-rich supernova remnant embedded in an H II region. The spectra show a blue continuum with a strong C IV $\lambda 1550$ P Cygni feature. Comparison to spectral standard stars observed with *IUE* shows similarities to O3-O7 V and early B Ia stars, indicating that massive young stars are present in the H II region. This comparison also indicates that the ultraviolet extinction in NGC 4449 may be peculiar. Careful inspection of the line-by-line data reveals a broad emission feature at 1657 Å that may be O III] emission from the supernova remnant. These observations are used in conjunction with shock model calculations to estimate limits on the relative abundances of carbon, silicon, and oxygen in the supernova remnant.

Subject headings: nebulae: abundances — nebulae: H II regions — nebulae: individual —
 nebulae: supernova remnants — ultraviolet: spectra

I. INTRODUCTION

Young supernova remnants (SNRs) that show abundance anomalies are of interest because they provide a unique opportunity to study nucleosynthesis and the way processed elements are returned to the interstellar medium. They can also be used to infer some of the characteristics of the precursor star, thus providing information on which stars explode and what kind of remnants they produce. Remnants that show a large abundance of oxygen, such as Cas A in our Galaxy (Chevalier and Kirshner 1979, and references therein) and N132D in the Large Magellanic Cloud (Lasker 1978, 1980), are usually identified as the products of the explosions of massive stars ($\geq 10 M_{\odot}$). The discovery of additional oxygen-rich remnants in our Galaxy (Goss *et al.* 1980), the Magellanic Clouds (Mathewson *et al.* 1980; Dopita, Tuohy, and Mathewson 1981), and NGC 4449 (Seaquist and Bignell 1978; Balick and Heckman 1978) has made it possible to study this class of objects in a meaningful way.

The SNR in the irregular galaxy NGC 4449 is a unique and important member of this class. It was first discovered in the radio by Seaquist and Bignell (1978), who estimated that the source was 25 times the luminosity of Cas A at 2 cm (assuming a distance of 5 Mpc; see Sandage and Tammann 1975). Early optical work by Balick and Heckman (1978) and Kirshner and Blair (1980; hereinafter Paper I) showed a composite spectrum with narrow lines belonging to an H II region, and broad lines (half-width $\sim 3500 \text{ km s}^{-1}$)

of forbidden oxygen which were identified with the SNR. The large radio luminosity and peculiar optical spectrum prompted an X-ray observation with *HEAO 2* and further optical work by Blair, Kirshner, and Winkler (1983; hereinafter Paper II). The source was detected in the single *Einstein* High Resolution Imager frame with an X-ray luminosity of $L_x \sim 10^{38} \text{ ergs s}^{-1}$. The new optical spectra detected lines of Ne and S in addition to O. By assuming that the X-ray spectrum of the object was similar to that of Cas A, a self-consistent scenario was developed for the object and its interaction with the surrounding H II region. A massive precursor star of order $25 M_{\odot}$ was suggested by several lines of argument. The model developed in Paper II implied an age for the SNR of 100–200 years, an estimate that appears to be confirmed now that stringent upper limits on the SNR's diameter ($\lesssim 0.07$ or $\lesssim 4 \text{ pc}$) have become available from radio measurements (de Bruyn 1983; Bignell and Seaquist 1983).

The NGC 4449 SNR is the youngest, most intrinsically luminous, and most distant member of the oxygen-rich SNR class. NGC 4449 lies near the North Galactic Pole, and using measurements of the optical Balmer lines from the H II region, $E(B-V) \approx 0.17$. Since potentially important lines of C, Si, Mg, and O are available in the ultraviolet, we decided to observe the remnant using the *International Ultraviolet Explorer Satellite (IUE)*. These observations are described in the next section and discussed in § III.

II. OBSERVATIONS

Although the NGC 4449 SNR is intrinsically very luminous, its large distance, small angular size, and moderate reddening make it a difficult target for *IUE*. A very accurate position is available from radio measurements [$\alpha(1950)$: $12^{\text{h}}25^{\text{m}}44^{\text{s}}.8$;

¹ Guest Observer with the *International Ultraviolet Explorer Satellite*, which is jointly operated by the U.S. National Aeronautics and Space Administration, the Science Research Council of the U.K., and the European Space Agency.

² NAS-NRC Postdoctoral Research Fellow.

TABLE 1
OBSERVING LOG OF SNR AND COMPARISON SPECTRA

Image No.	UT Date	Exposure Time (s)	Comments
SWP 13406	1981 Mar 4	26400	SNR
SWP 16275	1982 Feb 6	37200	SNR
LWR 10071	1981 Mar 4	7200	SNR
SWP 13466	1981 Mar 12	47400	Blank field, exposed during LWR 10126
SWP 13485	1981 Mar 16	22080	Blank field, exposed during LWR 10138

$\delta(1950)$: $44^{\circ}23'23''.3$; Bignell and Seaquist 1983], and the source was acquired by blind-offsetting from the nearby star SAO 44177. All observations were made at low dispersion (resolution = 6 \AA) with the large aperture. The details of the observations are given in Table 1. In addition, information on several blank exposures which were used to investigate camera background (see below) is also shown. Details of the *IUE* spacecraft and its performance can be found in Boggess *et al.* (1978a, b).

Initially, a 440 minute short-wavelength exposure and 120 minute long-wavelength exposure were obtained in March of 1981. Examination of the Goddard extraction of these images was somewhat discouraging, although a P Cygni profile at C IV $\lambda 1550$ and other possible stellar absorption features were present in the SWP image. However, the SNR is much smaller than the H II region in which it resides. The point spread function of *IUE* in conjunction with possible small guiding errors over such long exposures would imply that any contribution from the SNR should lie mainly in

two or perhaps three lines of the spectrum. Hence, the SWP spectrum was re-extracted two lines at a time using software available at the Center for Astrophysics that operates directly on the line-by-line file. Using this method, a feature centered at $\sim 1657 \text{ \AA}$ with full width near 7000 km s^{-1} was isolated in lines 26 and 27 of SWP 13406. No similar features were identified at other wavelengths or in other lines of the spectrum. Since oxygen lines dominate the optical spectrum of the remnant, it is tempting to identify this feature with O III] $\lambda 1664$ from the SNR. While the wavelength coincidence is not excellent, the broad optical components were seen to be blueshifted relative to the narrow H II region lines by 500 km s^{-1} (Balick and Heckman 1978) and the object could have been slightly off-center in the *IUE* large aperture. Also, it is difficult to determine the centroid of such a weak, broad feature to better than $\pm 2 \text{ \AA}$.

Because the spectrum was noisy and the suspected O III] feature was very weak, we obtained a second short-wavelength exposure (SWP 16275) in February of 1982. This image was searched in the same manner as discussed above and a similar feature was found, this time in lines 27 and 28 of the line-by-line file. This exposure was considerably longer than the first one (620 minutes), but the spectrum is still very noisy.

We have combined lines 26 and 27 of SWP 13406 and lines 27 and 28 of SWP 16275 to improve the signal-to-noise ratio. These combined data representing 17.7 hours of integration are shown in Figure 1 after particle hits have been removed and after smoothing over three pixels. The suspected SNR feature is indicated as are the anticipated positions of C III] $\lambda 1909$ and C IV $\lambda 1550$. At C IV, a P Cygni profile is seen that no doubt belongs to the underlying stellar component, while no broad SNR component is apparent. The features at roughly $\lambda 1875$ and $\lambda 1910$ are

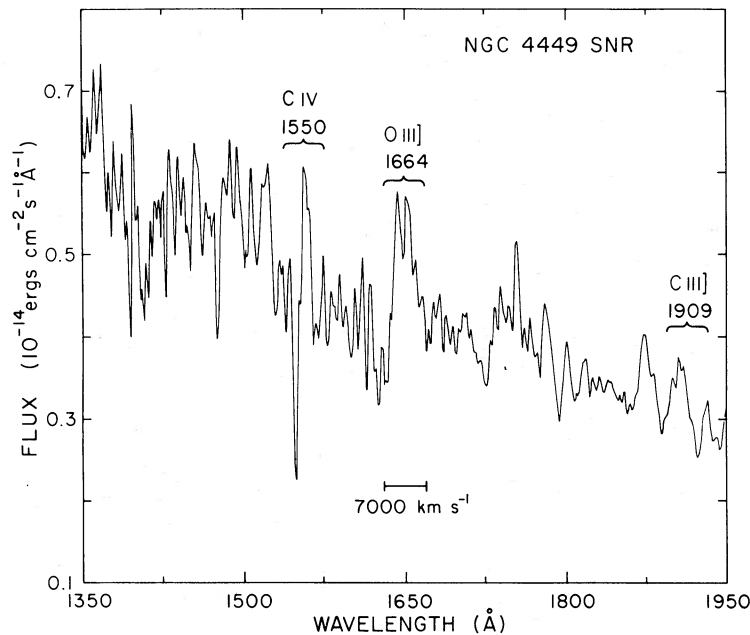


FIG. 1.—Short-wavelength *IUE* spectrum of the NGC 4449 SNR and accompanying H II region, obtained by adding lines 26 and 27 of SWP 13406 and lines 27 and 28 of SWP 16275. These lines were chosen to optimize the contribution of the proposed SNR feature at $\lambda 1657$ relative to the H II region background. The spectrum represents 17.7 hours of integration and has been smoothed over three pixels.

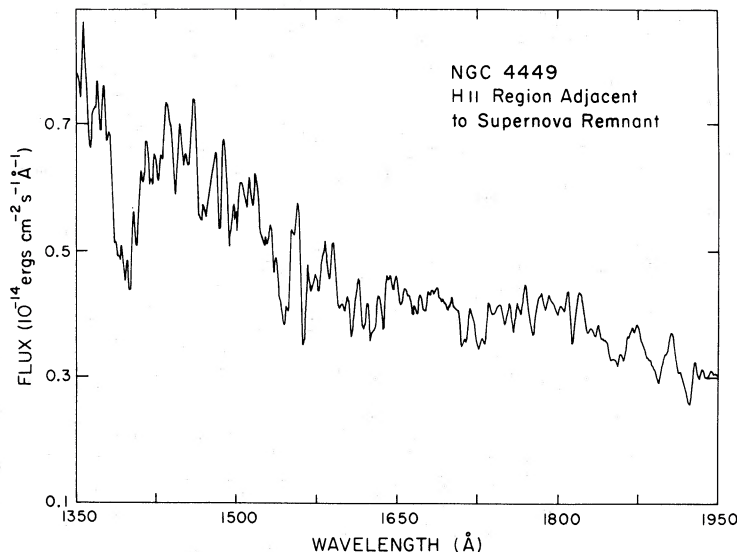


FIG. 2.—Short-wavelength *IUE* spectrum of the H II region component for comparison to Fig. 1. This spectrum was obtained by adding lines 24 and 25 of SWP 13406 to lines 25 and 26 of SWP 16275. Notice that the feature at $\lambda 1660$ has disappeared while the features of $\lambda 1875$ and $\lambda 1910$ are still present.

nearly at the expected positions of Si III] $\lambda 1887$ and C III] $\lambda 1909$; however, these are either camera features or they belong to the stellar component because they are not restricted to the same lines of the *IUE* spectra as the $\lambda 1664$ feature (see Fig. 2). Also, these features are narrower than would be expected from the SNR; their measured fluxes will be used as conservative upper limits on any SNR lines at these positions. The narrow emission line at $\lambda 1750$ is a “hot” camera pixel from line 27 that was present in both spectra before they were combined.

Figure 2 shows a spectrum obtained by summing the lines directly adjoining those that show the apparent SNR feature (i.e., lines 24 and 25 of SWP 13406 and lines 25 and 26 of SWP 16275). The $\lambda 1664$ feature is no longer present, although the $\lambda 1875$ and $\lambda 1910$ features remain.

We have also examined two long-exposure blank images from *IUE* that were obtained at about this time (see Table 1) in order to investigate the reality of this feature. These images were re-extracted two lines at a time and compared to the corresponding spectra from SWP 13406 and SWP 16275. A number of camera features were identified in this manner; the most important for our purposes are a reseau mark in lines 20 to 22 at 1661 \AA and a “hot spot” of six pixels (2×3) at 1663 \AA , which was found in lines 29 and 30 with a peak intensity of roughly $3 \times 10^{-15} \text{ ergs cm}^{-2} \text{ s}^{-1} \text{ \AA}^{-1}$. These features are much narrower than the suspected SNR line, and they are not in the same two lines of the *IUE* image. Figure 3 shows the sum of lines 26 through 28 from one of the blank field exposures for comparison to Figure 1. No camera features were identified in the $1600\text{--}1700 \text{ \AA}$ region of the comparison images. In addition, there are no stellar features that can account for the observations (see below), and no such feature is seen in *IUE* spectra of blue irregular galaxies (Huchra *et al.* 1983).

We believe that the procedure followed has established the reality of the emission feature, and that this feature can be identified with the O III] $\lambda 1664$ line from the SNR. However,

the absolute flux is uncertain by at least 50% because the noise in the spectrum is still considerable and because the baseline is very uncertain. The measured flux of this feature and upper limits on other possible SNR lines are listed in Table 2.

The long-wavelength spectrum LWR 10071 was exposed for only two hours, and it is very noisy, especially at the short-wavelength end. However, by combining data from lines

TABLE 2
COMPARISON OF NGC 4449 SNR OBSERVATIONS TO
SHOCK MODEL CALCULATIONS

LINE ID	λ (Å)	NGC 4449 SNR		ITOH ^b MODEL C	EXTENDED MODEL C ^c
		$F(\lambda)$	$I(\lambda)^a$		
Ultraviolet:					
Si IV, (O IV)	1400	<10	<30	(3.7)	120
C IV	1550	<12	<42	...	99
O III]	1664	20.1	36.4	36.0	36.4
Si III]	1887	<6.5	<23	...	58.3
C III]	1909	<6.1	<22	...	155
Mg II	2800	<65	<170
Optical ^d :					
[O II]	3727	7.7	9.5	25.7	...
[Ne III]	3869, 3968	9.9	12
[S II]	4069, 4075	3.9	4.6
[O III]	4363	6.5	7.2	9.2	...
[O III]	4959, 5007	100 ^e	100 ^f	100	...
[O I]	6300, 6363	24	20	82	...
[O II]	7320, 7330	54	38	17	...

^a Reddening correction assumes $E(B-V) = 0.17$ and extinction curve from Seaton 1979.

^b Pure oxygen model from Itoh 1981 with preshock density $n_e = 10^3 \text{ cm}^{-3}$ and $v_s = 141 \text{ km s}^{-1}$.

^c See text.

^d Optical data from Blair *et al.* 1983.

^e $F(\text{O III}) = 2.02 \times 10^{-13} \text{ ergs cm}^{-2} \text{ s}^{-1}$.

^f $I(\text{O III}) = 3.79 \times 10^{-13} \text{ ergs cm}^{-2} \text{ s}^{-1}$.

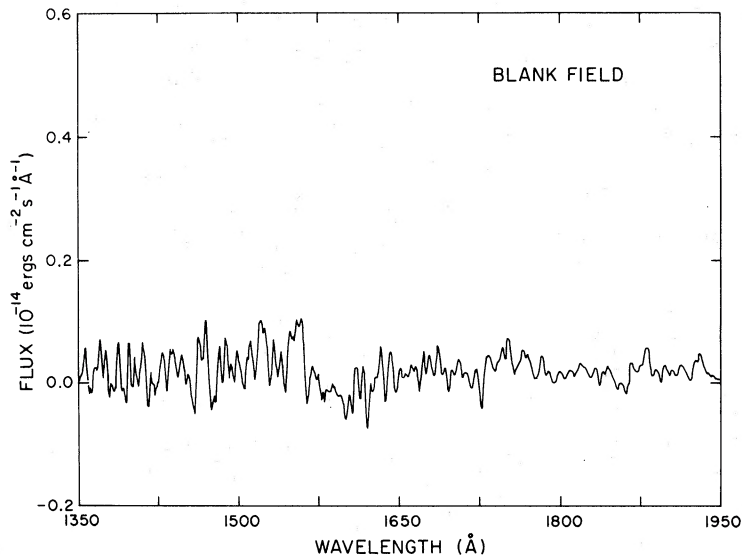


FIG. 3.—Lines 26 through 28 from the long, blank field exposure SWP 13466, for comparison to Fig. 1. This exposure was obtained near in time to the first SNR exposure (SWP 13406) and shows that there were no camera features that can account for the proposed SNR line.

25 to 30 (where the majority of the H II region emission arises) for both short and long wavelength exposures, and binning the data into 50 Å averages, a reasonable representation of the continuum shape from 1250 to 3200 Å can be obtained. If this continuum is dereddened using the extinction formulation of Seaton (1979) and $E(B-V)$ from the Balmer lines, an apparent excess of emission is found in the 2000–2300 Å range. This could indicate that the reddening is somewhat less than indicated by the Balmer lines; indeed the region around 2200 Å is consistent with there being no extinction. However, since most of the extinction is probably intrinsic to NGC 4449, it could be that the mean galactic extinction curve is not appropriate.

The extinction along some lines of sight in the Large Magellanic Cloud (LMC) has been shown to be peculiar, especially around the 30 Doradus region (Nandy *et al.* 1980). Since NGC 4449 is classified as a Magellanic irregular galaxy, it may also exhibit peculiar extinction properties. The observed anomalies in the LMC are in the correct sense to explain the discrepancy observed in NGC 4449: the extinction law in the 30 Dor region is much smoother, and the 2200 Å feature is much less distinct. However, since the extinction law changes from place to place within the LMC, it may not be appropriate to apply the 30 Dor extinction law to NGC 4449 without further information.

The underlying stellar component can also be used to shed some light on the extinction situation. Comparison of the data from lines 25 to 30 with the IUE spectral atlas recently compiled by Wu *et al.* (1981) allows a number of stellar features to be identified, some of which are also visible in Figure 1. No single spectrum provides an entirely satisfactory match, although this might be expected since the combined light of many stars is entering the spectrograph slit. In general, C IV P Cygni profiles with emission components comparable in strength with the absorption components are seen only in the middle O V stars. There are a number of

broad absorption features in these comparison spectra in the 1250–1350 Å range and at 1725 Å that may also be present in our spectrum. The overall choppiness of the continuum with broad absorptions around $\lambda\lambda$ 1300, 1400, 1625, and 1725 is also reminiscent of late O and early B Ia comparison spectra. Whatever the detailed makeup of the underlying stellar component is, it is clearly dominated by the presence of massive O and B stars; this is consistent with the argument presented in Paper I based on the absolute flux in the H β line. Comparing the slope of our observed continuum to some of these spectral standards (excluding the 2000–2300 Å region), we find it necessary to deredden the observations using $E(B-V) = 0.25$, which is somewhat higher than that indicated by the Balmer lines and much higher than found from the λ 2200 feature. This comparison could be affected by the presence of cooler stars as well as any peculiarities in the extinction along this line of sight. Given these inconsistencies, we will use the value of $E(B-V)$ indicated by the Balmer lines and the extinction curve of Seaton (1979) to obtain reddening-corrected fluxes for comparisons to model calculations. These values are also shown in Table 2.

III. DISCUSSION

Shock model calculations for a range of physical conditions and roughly cosmic abundances have been available for some years (Cox 1972; Dopita 1977; Raymond 1979; Shull and McKee 1979). The use of these models in conjunction with both IUE and optical observations of SNRs (e.g., Benvenuti, Dopita, and D'Odorico 1980; Raymond *et al.* 1981; Fesen, Blair, and Kirshner 1982, and references therein) has proven to be an important diagnostic tool. Both observations and models show that C III] λ 1909 and C IV λ 1550 are the strongest ultraviolet lines expected from these “normal” abundance situations, followed closely by O III] λ 1664, O IV] + Si IV λ 1400, Si III λ 1887, He II λ 1640, and lines of nitrogen. The abundances in the NGC 4449 SNR are not

expected to be anything like cosmic abundances (cf. Paper II), but the absence of these lines which are normally stronger or comparable to O III] $\lambda 1664$ may provide constraints on the abundances of other elements relative to oxygen.

The material in the NGC 4449 SNR appears to be largely oxygen, with other elements present as trace constituents. The heating and cooling mechanisms in such a gas are sufficiently different from the standard H and He dominated case that the shock models mentioned above are of limited usefulness. Recently, Itoh (1981) has calculated some shock models assuming a pure oxygen gas and has discussed some of the differences between this case and that of normal abundances. With a limited sampling of parameter space, Itoh was able to explain the observed optical line intensities of the oxygen knot in Cas A (Chevalier and Kirshner 1979) and knot B of N132D (Lasker 1978) but was unable to find a match for the NGC 4449 SNR. In Table 2 we show Itoh's model C, which has a shock velocity of 141 km s^{-1} and the highest preshock density ($n_e = 10^3 \text{ cm}^{-3}$) of any of his models. This is still not a high enough density to collisionally de-excite [O II] $\lambda 3727$ to the level observed in the NGC 4449 SNR; in Paper II, we estimated $n_e \sim 3 \times 10^5 \text{ cm}^{-3}$ in the postshock O^+ zone.

Itoh's models indicate that O III] $\lambda 1664$ is expected to be the strongest ultraviolet oxygen line. In Table 2, we see that the observed feature is about the right strength relative to [O III] $\lambda \lambda 4959, 5007$, although the extent of the agreement is fortuitous given the uncertainties of measuring weak, broad features relative to a noisy background, and the uncertainty in extinction.

In order to obtain upper limits on the abundances of carbon and silicon from the upper limits on their emission lines, we require a model for the strengths of these lines. The structure of the ultraviolet emitting region in Itoh's model C is extremely simple. Because the electron and ion temperatures are assumed to equilibrate only through Coulomb collisions and because the radiative cooling rate of the pure oxygen gas is extremely large, the electron temperature stays constant at just over 10^5 K (see Itoh's Fig. 5). This temperature is determined by the balance between energy losses due to excitation of the oxygen ions and energy gains due to elastic collisions with the ions. The electrons remain at this temperature over a distance of about 10^{12} cm , at which point the thermal energy is exhausted and the temperature drops suddenly. The trailing photoionization zone can produce significant optical radiation, but it is too cool to contribute significantly to the UV lines.

To compute the intensities of Si and C lines in this model, we assume $T_e = 10^{5.1} \text{ K}$ from Itoh's Figure 5 and calculate the time-dependent ionization structures of C, O, and Si. Ionization and recombination coefficients were as described in Raymond (1979). Collision strengths for the UV lines were taken from Baluja, Burke, and Kingston (1980, 1981), Dufton *et al.* (1978), Hayes (1982), and Merts *et al.* (1980). All were close coupling calculations, and all the intercombination excitations include the contribution of resonances, so we expect these collision strengths to be quite accurate. Predicted ultraviolet line intensities assuming solar abundances relative to O (from Allen 1973) are given in Table 2, scaled relative to the observed O III] line. Our predicted O III] intensity is 20% lower than Itoh's, indicating

TABLE 3
ABUNDANCE ESTIMATES COMPARED TO
NUCLEOSYNTHESIS MODELS

Ratio ^a	NGC 4449 SNR	15 M_{\odot} ^b Model	25 M_{\odot} ^b Model
C/O	<0.3	1.0	0.42
Si/O	<0.25	2.7-3.8	0.8-1.3
S/O	0.6 ^c	1.2	0.7
Ne/O	1.37 ^c	3.63	1.77

^a Ratios are for abundances by number, scaled relative to the corresponding ratios in the sun, assuming solar abundances from Allen 1973.

^b From Weaver and Woosley 1980.

^c From Blair *et al.* 1983.

that there are no major differences between our calculations. This also shows that O is still the main coolant and implies that the addition of C and Si has not significantly affected the simple structure of the cooling zone.

The ultraviolet observations also provide a constraint on the shock velocity. Within the context of the Coulomb equilibration model, increasing the shock velocity, v_s , by $2^{1/2}$ would double the ion temperature. This would also approximately double the electron temperature. The cooling time would stay about the same, since the increased thermal energy content of the gas would balance the increased cooling rate. We find that such a shock would have an O IV] $\lambda 1400$ feature twice as strong as the O III] $\lambda 1664$ line. Thus, the lack of detectable O IV] emission implies $v_s < 200 \text{ km s}^{-1}$.

The observational upper limits on the C and Si lines are considerably smaller than those predicted from the extended Itoh model. Assuming that these lines scale relative to O III] with abundances, we can use the upper limits to derive rough limits on the abundances of C and Si relative to O. These limits are shown in Table 3, scaled relative to the corresponding abundance ratios seen in the Sun. The value shown for C/O is an average of the values obtained from C III]/O III] and C IV]/O III], since the ionization potentials of these C ions bracket that of O^{++} . The value for Si/O is derived from the Si IV]/O III] ratio because the Si^{+3} ionization potential is closer to O^{++} than is Si^{++} . For completeness, we also show the values for S and Ne relative to O as derived in Paper II.

Weaver and Woosley (1980) have constructed complete evolutionary models of $15 M_{\odot}$ and $25 M_{\odot}$ stars that follow the stars from zero-age main sequence through core collapse and the ensuing explosion. While these models neglect mass loss and rotation effects, they do include explosive nucleosynthesis and predict the relative abundances that would be ejected by the supernova explosion. Weaver and Woosley find that elements from O to Mg are largely unmodified by the explosion while elements from Si to Fe can be produced explosively. The range of values for Si in Table 3 shows the results for their low and high energy explosions, respectively.

As was found for Ne and S in Paper II, the observed limits for C and Si lie outside the range of the model predictions. However, if we linearly extrapolate the $15 M_{\odot}$ and $25 M_{\odot}$ results to slightly higher masses, we find that a precursor star of $\sim 30 M_{\odot}$ would satisfy all of the observational

constraints. Such an extrapolation is perhaps not strictly valid, but it is interesting and encouraging that the limits supplied by the ultraviolet measurements are consistent with, and even supportive of, the results derived in Paper II.

It is a pleasure to thank the *IUE* Observatory staff for their assistance and patience during the observations. This work was supported by NASA grants NAG 5-87 and NAGW-117 to the Smithsonian Astrophysical Observatory.

REFERENCES

- Allen, C. W. 1973, *Astrophysical Quantities* (3d ed.; London: Athlone).
 Balick, B., and Heckman, T. 1978, *Ap. J. (Letters)*, **226**, L7.
 Baluja, K. L., Burke, P. G., and Kingston, A. E. 1980, *J. Phys. B*, **13**, 829.
 ———, 1981, *J. Phys. B*, **14**, 1333.
 Benvenuti, P., Dopita, M., and D'Odorico, S. 1980, *Ap. J.*, **238**, 601.
 Bignell, R. C., and Seaquist, E. R. 1983, *Ap. J.*, **270**, 140.
 Blair, W. P., Kirshner, R. P., and Winkler, P. F. 1983, *Ap. J.*, **272**, 84 (Paper II).
 Boggess, A., et al. 1978a, *Nature*, **275**, 372.
 Boggess, A., et al. 1978b, *Nature*, **275**, 377.
 Chevalier, R. A., and Kirshner, R. P. 1979, *Ap. J.*, **233**, 154.
 Cox, D. 1972, *Ap. J.*, **178**, 143.
 de Bruyn, A. G. 1983, *Astr. Ap.*, **119**, 301.
 Dopita, M. A. 1977, *Ap. J. Suppl.*, **33**, 437.
 Dopita, M. A., Tuohy, I. R., and Mathewson, D. S. 1981, *Ap. J. (Letters)*, **248**, L105.
 Dufton, P. L., Berrington, K. A., Burke, P. G., and Kingston, A. E. 1978, *Astr. Ap.*, **62**, 111.
 Fesen, R. A., Blair, W. P., and Kirshner, R. P. 1982, *Ap. J.*, **262**, 171.
 Goss, W. M., Ekers, R. D., Danziger, I. J., and Israel, F. P. 1980, *M.N.R.A.S.*, **193**, 901.
 Hayes, M. A. 1982, *M.N.R.A.S.*, **199**, 49P.
 Huchra, J. P., Geller, M. J., Gallagher, J., Hunter, D., Hartmann, L., Fabbiano, G., and Aaronson, M. 1983, *Ap. J.*, **274**, 125.
 Itoh, H. 1981, *Pub. Astr. Soc. Japan*, **33**, 1.
 Kirshner, R. P., and Blair, W. P. 1980, *Ap. J.*, **236**, 135 (Paper I).
 Lasker, B. 1978, *Ap. J.*, **223**, 109.
 ———, 1980, *Ap. J.*, **237**, 765.
 Mathewson, D. S., Dopita, M. A., Tuohy, I. R., and Ford, V. L. 1980, *Ap. J. (Letters)*, **242**, L73.
 Merts, A. L., Mann, J. B., Robb, W. D., and Magee, N. H., Jr. 1980, Los Alamos Informal Report LA-8267-MS.
 Nandy, K., Morgan, D. H., Willis, A. J., Wilson, R., Gondhalekar, P. M., and Houziaux, L. 1980, *Nature*, **283**, 725.
 Raymond, J. C. 1979, *Ap. J. Suppl.*, **39**, 1.
 Raymond, J. C., Black, J. H., Dupree, A. K., Hartmann, L., and Wolff, R. S. 1981, *Ap. J.*, **246**, 100.
 Sandage, A., and Tammann, G. A. 1975, *Ap. J.*, **196**, 313.
 Seaquist, E. R., and Bignell, R. C. 1978, *Ap. J. (Letters)*, **226**, L5.
 Seaton, M. 1979, *M.N.R.A.S.*, **187**, 73P.
 Shull, J. M., and McKee, C. F. 1979, *Ap. J.*, **227**, 131.
 Weaver, T. A., and Woosley, S. E. 1980, *Ann. N.Y. Acad. Sci.*, **336**, 335.
 Wu, C.-C., Boggess, A., Holm, A. V., Schiffer, F. H., and Turnrose, B. E. 1981, *IUE Ultraviolet Spectral Atlas* (Greenbelt: Goddard Space Flight Center), preliminary edition.

WILLIAM P. BLAIR and JOHN C. RAYMOND: Harvard-Smithsonian Center for Astrophysics, 60 Garden Street, Cambridge, MA 02138

ROBERT A. FESEN and THEODORE R. GULL: Laboratory for Astronomy and Solar Physics, NASA Goddard Space Flight Center, Code 685, Greenbelt, MD 20771